Determination of Order Parameters in Laterally Fluorosubstituted Terphenyls by ^{19}F-NMR, Optical and Dielectric Anisotropies

M. Geppi [a] , A. Marini [a] , B. Mennucci [a] , P. Kula [b] , A. Spadło [b] , W. Kuczyński [c] & S. Urban [d]

[a] Department of Chemistry and Industrial Chemistry, University of Pisa, Pisa, Italy

[b] Institute of Chemistry, Military University of Technology, Warsaw, Poland

[c] Institute of Molecular Physics, Polish Academy of Sciences, Smoluchowskiego, Poznań, Poland

[d] Institute of Physics, Jagiellonian University, Krakow, Poland

PLEASE SCROLL DOWN FOR ARTICLE

demand, or costs or damages whatsoever or howsoever caused arising directly or indirectly in connection with or arising out of the use of this material.

Taylor & Francis
Taylor & Francis Group

Determination of Order Parameters in Laterally Fluorosubstituted Terphenyls by ^{19}F-NMR, Optical and Dielectric Anisotropies

M. GEPPI,[1] A. MARINI,[1] B. MENNUCCI,[1] P. KULA,[2]
A. SPADŁO,[2] W. KUCZYŃSKI,[3] AND S. URBAN[4]

[1]Department of Chemistry and Industrial Chemistry, University of Pisa, Pisa, Italy
[2]Institute of Chemistry, Military University of Technology, Warsaw, Poland
[3]Institute of Molecular Physics, Polish Academy of Sciences, Smoluchowskiego, Poznań, Poland
[4]Institute of Physics, Jagiellonian University, Krakow, Poland

Orientational order parameter in five fluorinated nematogens have been investigated by means of optical, dielectric and ^{19}F NMR techniques. Quantum mechanical calculations were also employed to derive molecular and nuclear properties necessary for the analysis of the spectroscopic quantities. The obtained data were compared and discussed taking into account the differences among the three methods. The values of the order parameter differ due to different anisotropic physical quantities measured and, consequently, the different axes frame in which the order parameters are defined. However, the temperature trends, expressed with the aid of the Haller-type relation, are very close within the broad range of the nematic phase.

1. Introduction

Many experimental techniques can be employed in determining the orientational order parameters in liquid crystal (LC) phases [1]. Among them the nuclear magnetic resonance (NMR) technique is commonly considered as the best tool for that purpose, first of all because of the straightforward relation between measured nuclear properties and order parameters. Different anisotropic interactions (e.g., quadrupolar, dipolar, chemical shift) and nuclei (e.g., ^{2}H, ^{13}C, ^{19}F) can be exploited to derive local order parameters by means of NMR techniques [2]. In some cases, however, in order to determine fragment or molecular order parameters, additional information on molecular geometry and nuclear properties (e.g., chemical shift tensors) are

---

*This paper is dedicated to the memory of our friend and colleague Alberto Marini.

Address correspondence to Prof. S. Urban, Institute of Physics, Jagiellonian University, 30-059 Krakow, Poland. E-mail: ufurban@cyf-kr.edu.pl

needed, and to this purpose density functional theory (DFT) calculations can be exploited [3–5]. On the other side, optical birefringence and dielectric anisotropy methods, which are related to the principal axis of the polarizability tensor and molecular dipole moment, respectively, must be analysed in terms of the appropriate theoretical models to derive ''molecular'' order parameters. The combination of these three methods has already proved to be successful in the investigation of orientational order properties of liquid crystals. Indeed, a common discussion of the data determined by these three techniques does allow a better understanding of the molecular arrangements in LC phases and it represents a severe test for the theoretical models applied [3–5].

The results obtained by these three methods (NMR, optical birefringence and dielectric anisotropy) for selected fluorosubstituted terphenyls with structures:
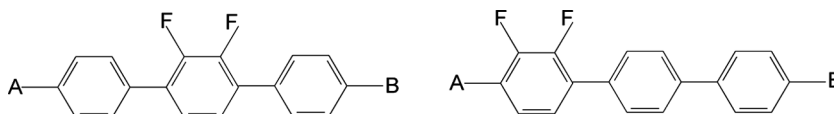
where A means alkyl, and B alkyl or alkoxy groups, are presented in this paper. These compounds were recently synthesised in the Military University of Technology, Warsaw [6]. Their dielectric properties (static and dynamic) were already reported in ref. [7]. These compounds exhibit a negative dielectric anisotropy ($\Delta\varepsilon = \varepsilon_\parallel - \varepsilon_\perp < 0$), contrary to previously studied fluorinated compounds with the positive dielectric anisotropy [3,5].

[19]F nuclei have been here extensively used for determining the orientational order parameters by NMR. Dielectric anisotropy was analysed taking into consideration the well known Maier and Meier equation. Optical anisotropy was measured by the method described in ref. [8]. The differences among the order parameters obtained by the three methods are discussed in detail, also with reference to the assumptions and approximations used in each case.

The aim of this research work is to find possible correlations between the principal orientational order parameters (S_{zz}) and the position of the laterally attached fluorine atoms, as well as the types and length of the terminal chains, getting insights into the structure-property relationships, in the perspective of understanding how to tailor the properties of these materials in function of their chemical structure.
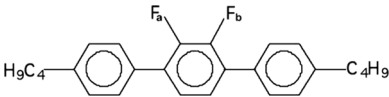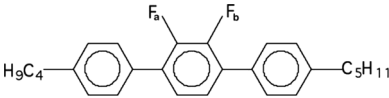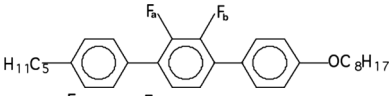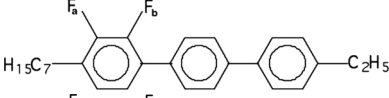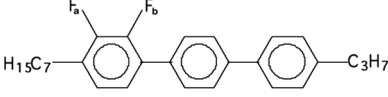
2. Experimental

The terphenyls studied in the present work are listed in Table 1 along with their mesomorphic temperature ranges. The abbreviations are the same as those used in ref. [7].

2.1. *Dielectric and Optical Studies*

The tensor permittivity components in the nematic phase, $\varepsilon_\parallel$ and $\varepsilon_\perp$, were determined as described in ref. [7]. The samples were oriented by a magnetic field of 0.7 T. In all cases the measurements started in the isotropic phase and the samples were cooled down step by step, which led to supercooling effect. The optical birefringence,

Table 1. Chemical structures and transition temperatures (in °C) of the substances studied. The abbreviations are the same as those used in ref. [7]

Acronym	Chemical structure	Phase diagram [°C]
KS 2	H_9C_4—◯—◯(F_a, F_b)—◯—C_4H_9	Cr 67 N 102 Is
KS 7	H_9C_4—◯—◯(F_a, F_b)—◯—C_5H_{11}	Cr 50.8 N 111.6 I
KS 9	$H_{11}C_5$—◯—◯(F_a, F_b)—◯—OC_8H_{17}	Cr 47.7 S_C 96.3 N 142.2 I
KS 12	$H_{15}C_7$—◯(F_a, F_b)—◯—◯—C_2H_5	Cr 66.2 S_C 78.7 N 126 I
KS 13	$H_{15}C_7$—◯(F_a, F_b)—◯—◯—C_3H_7	Cr 86.6 S_C 96.4 S_A 119.4 N 138 I

$\Delta n = n_e - n_o$, in the nematic phase was measured by the method described in ref. [8]. The measuring cell composed of a glass plate and a convex lens had a variable thickness. It was filled with the samples in the isotropic phase and cooled down to the nematic phase. The sample was placed between crossed polarizers on a microscope stage. In this arrangement a system of circular interference fringes was observed – see Figure 1. From the diameters of fringes the optical birefringence Δn could be calculated.
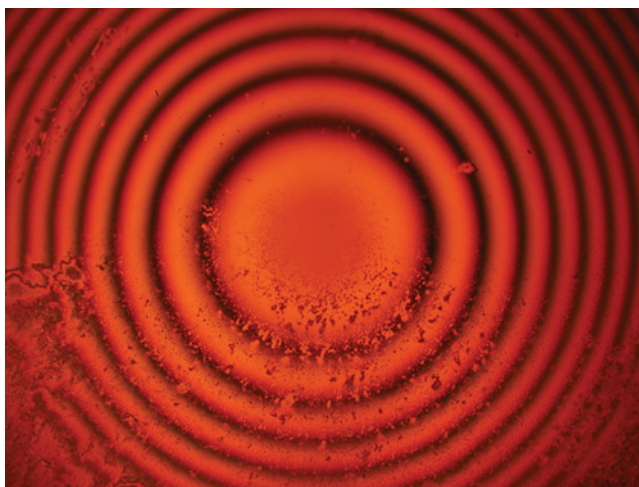
Figure 1. Interference fringes observed in the nematic phase of KS 2. (Figure appears in color online.)

2.2. ^{19}F NMR Measurements

^{19}F NMR spectra on neat terphenyls were recorded on a Varian Unity 300 spectrometer working at 282.23 MHz for ^{19}F, equipped with a 5-mm probe. The ^{19}F 90° pulse length was 15.0 µs, and 300–600 transients were accumulated, depending on the available sample quantity, with a recycle delay of 0.3 s. The chemical shift scale in the mesophases was referred to the chemical shift of the fluorine nucleus with the lowest resonance frequency in the isotropic phase, arbitrarily put equal to zero. For the ^{19}F measurements in the mesophases, the samples were uniformly aligned by slow cooling from the isotropic to the liquid crystalline phase within the magnetic field. Spectra were recorded on cooling. The temperature was stable within ±0.2 K.

2.3. DFT Calculations

The quantum-mechanical calculations, performed by using the Gaussian 09 package (version A.01) [9] were done on both the full-molecule models of several terphenyl systems (KS), shown in Table 1, and their simplified models (mKS), where the alkyl chains were replaced with methyl groups.

The geometry optimizations were performed at DFT level of theory, employing the combination of B3LYP [10] functional with the 6-311G(d) basis set. The calculations were done for an isolated molecule (in vacuo) and by taking into account the effect of an anisotropic environment with the IEF-PCM model [11]. The vibrational frequencies calculations, performed at the same level of theory used for the geometry optimizations, were employed to check if the obtained structures effectively represented minimum energy conformers for the systems studied.

The PCM cavities were built from radii obtained by applying the United Atom Topological Model to the atomic radii of the UFF force field [12] as implemented in the Gaussian 09 code (using the keyword G03defaults).

For both geometry optimizations and vibrational frequencies calculations, the experimental isotropic dielectric permittivities (ε^{iso}) values of 4.3, 4.3, 4.1, 4.3 and 3.9 were used for KS2, KS7, KS9, KS12 and KS13, respectively. The ε^{iso} values were taken in the middle of the mesomorphic temperature range of the investigated compounds. The use of different values of ε^{iso}, for instance taken at the Iso-N or N-Cr transition temperatures, did not introduce significant changes in the molecular geometry.

Fluorine-19 chemical shielding tensors (CSTs) were calculated by the method of Gauge-Including Atomic Orbitals, GIAO [13] and using the modified Perdew-Wang [14] exchange-correlation functional, called MPW1PW91 [15] in combination with the 6–311 + G(d,p) basis set. For CST calculations the experimental values of 4.6, 4.7, 4.5, 4.6 and 4.2 for the perpendicular, $\varepsilon_\perp$, and the values of 3.6, 3.6, 3.4, 3.6 and 3.4 for the parallel, $\varepsilon_\parallel$, components of the dielectric permittivity tensor were used for KS2, KS7, KS9, KS12 and KS13, respectively.

Finally, the computed fluorine-19 absolute chemical shielding values (σ scale) were converted in the corresponding traceless chemical shifts (δ shift scale), by subtracting them from the isotropic chemical shielding value.

For our convenience, the labels "VACUO Mod", "VACUO" and "ANISO" will indicate the ^{19}F CSTs (as well as the corresponding S_{zz} parameters) calculated in vacuo for the simplified models (mKS), in vacuo and in the medium (liquid crystalline phase, by using IEF-PCM calculations) for the full molecules, respectively.

3. Results

3.1. *Optical and Dielectric Spectroscopy Studies*

The temperature dependence of Δn, reported in Figure 2 for the therphenyls investigated in this work, was fitted to the experimental points by following a Haller-type formula [16]:

$$\Delta n = \delta n \left(1 - \frac{T}{T^*} \right)^{\beta} \tag{1}$$

where δn, T^* and β are fitting parameters and $S(T) = \Delta n(T)/\delta n$.

Dielectric anisotropy, $\Delta \varepsilon = \varepsilon_\parallel - \varepsilon_\perp$, was measured for all the investigated compounds (see Fig. 3) and it was analyzed using the Maier and Meier equation [17]:

$$\Delta \varepsilon = \varepsilon_\parallel - \varepsilon_\perp = \varepsilon_0^{-1} N_0 h F \left[\Delta \alpha - F \frac{\mu^2}{2kT} \left(1 - 3\cos^2 \beta \right) \right] S \tag{2}$$

where $N_0 = N_A \rho / M$, N_A – Avogadro's number, ρ is the density and M the molar mass, ε_0 – the permittivity of free space, h, F – local field factors dependent upon the mean dielectric permittivity $<\varepsilon> = (\varepsilon_\parallel + 2\varepsilon_\perp)/3$, $\Delta \alpha$ – polarizability anisotropy, β – angle between the dipole moment μ and the long axis, $S = <1 - 3\cos^2\theta>/2$ – order parameter, θ – angle between the molecular axis and the director. For the substances studied $\beta \sim 90°$, see ref. [7].

For all terphenyls the dipolar part in the Maier and Meier equation is markedly larger than the polarizability anisotropy: $\Delta \alpha \sim 20\,\text{Å}^3$ (estimated, see Appendix), whereas $F\mu^2/2kT \approx 90\,\text{Å}^3$. In that situation the following simplification: $S(T) \sim T\Delta \varepsilon(T)/hF^2$ seems to be acceptable (density changes with temperature scarcely in comparison with $\Delta \varepsilon(T)$). Additionally, it was assumed $S(T) = S_o(\Delta T)^{\gamma}$ with $S_o = 1/T^{\gamma}_{NI}$.
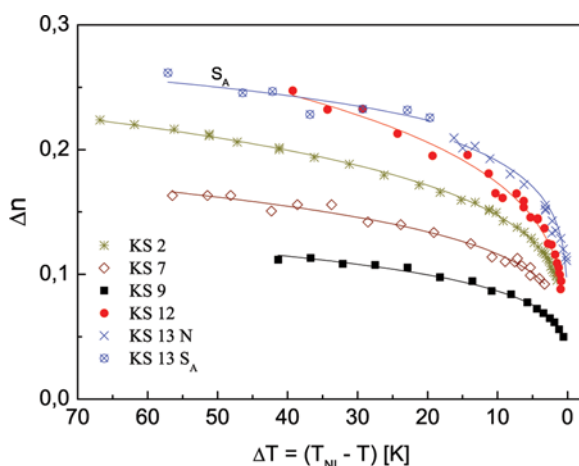

Figure 2. Optical birefringence *vs.* shifted temperature collected for the five investigated substances. (Figure appears in color online.)
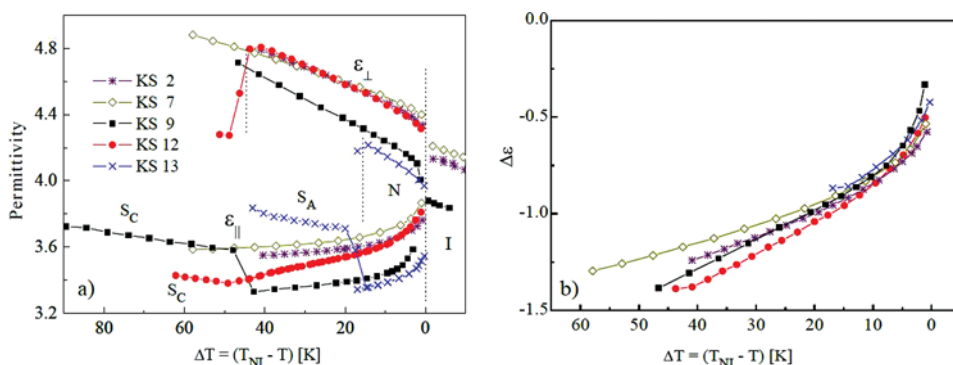
Figure 3. Static dielectric permittivity components (a) and the dielectric anisotropy $\Delta\varepsilon = \varepsilon_\parallel - \varepsilon_\perp$(b) *vs.* shifted temperature for the five investigated substances. (Figure appears in color online.)

3.2. ^{19}F NMR Study

Static ^{19}F NMR spectra were recorded for each liquid crystal in its isotropic melt state, as well as in its whole mesomorphic temperature range. A selection of them is reported in Figure 4. The spectra recorded for the different samples in the isotropic phase show one or two peaks depending on the number of inequivalent ^{19}F nuclei, in turns affected by the symmetry of the molecule. The spectra recorded in the
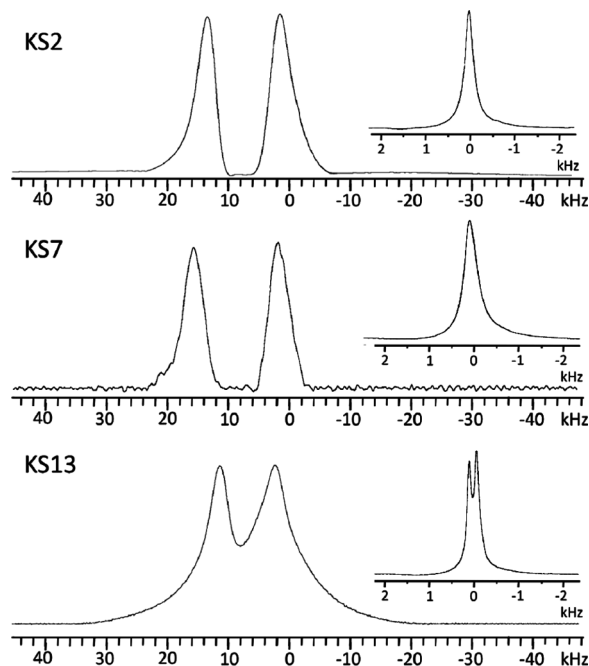

Figure 4. Static and isotropic (in the insets) ^{19}F spectra of KS2, KS7 and KS13, recorded in their nematic phases at 85°C, 88°C and 128°C, and in their isotropic melt phases at 110°C, 120°C and 142°C, respectively.

mesophases are characterized, for all the samples, by the presence of a doublet, due to ^1H-^{19}F dipolar splitting. In particular, the spectrum of KS2 in the isotropic phase shows a single peak, reflecting the symmetry of the molecule; a similar situation is observed for KS7 and KS9 (spectrum not shown) even though the molecular structure of these compounds is asymmetric, indicating that the electronic densities surrounding F_a and F_b (which are located on the central aromatic ring) are negligibly affected by the presence of different aliphatic chains. On the contrary, in KS13 and KS12 (spectrum not shown) F_a and F_b, belonging to a lateral aromatic ring, are more strongly inequivalent, resulting in two well distinguished peaks in the ^{19}F spectrum recorded in the isotropic phase and in broader and more asymmetric lines of the dipolar doublet observed in the mesophase.

In Figure 5 we reported the ^{19}F chemical shift anisotropies, $\delta^{aniso} = \delta^{obs} - \delta^{iso}$, extracted at different temperatures subtracting the isotropic chemical shift measured in the melt phase (or the average of the two isotropic chemical shifts in KS12 and KS13) from the chemical shift of the center of mass of the dipolar doublets measured in the mesophases. For the sake of simplicity, for each sample the zero of the chemical shift scale was taken as the resonance frequency of the single isotropic peak (for KS2, KS7 and KS9) or as the average of the two isotropic peaks (for KS12 and KS13). All this considered, being $\delta^{iso} = 0$, the shifts observed in the mesophase directly corresponds to the anisotropic shift, $\delta^{aniso} = \delta^{obs}$, which can be analyzed to derive the principal orientational order parameters S_{zz} through the following equation, where biaxiality has been neglected:

$$\delta^{aniso} = \frac{2}{3}\left[\delta_{zz} - (\delta_{xx} + \delta_{yy})/2\right] \cdot S_{zz} = \frac{2}{3}\Delta\delta \cdot S_{zz} \qquad (3)$$
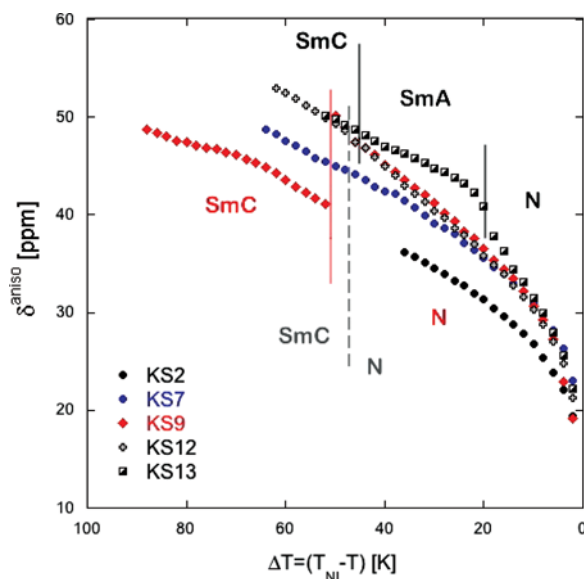

Figure 5. Trends of the ^{19}F chemical shift anisotropies δ^{aniso} (ppm) vs. reduced temperature $\Delta T = T_{NI} - T$ (K) for the terphenyls investigated in this study. The inter-mesophase transitions for KS9, KS12 and KS13 are indicated by red (solid), grey (dashed) and black (solid) lines, respectively. (Figure appears in color online.)
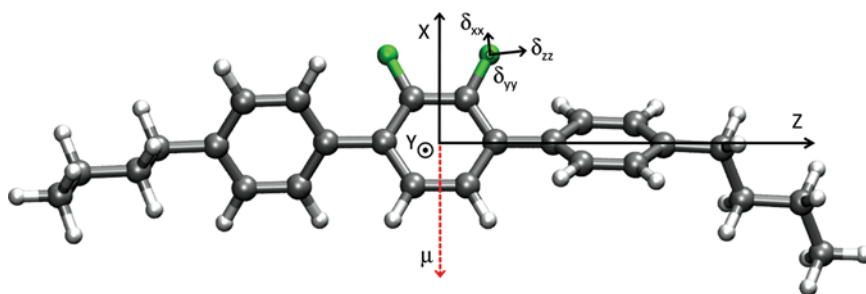
Figure 6. Reference axes frame for the calculations of the dipole moments, the ^{19}F chemical shielding tensors and the principal orientational order parameter, S_{zz}, of the investigated compounds. The molecular structure of KS2 is reported here as an example, together with the location of the dipole moment vector (μ) and the principal axes frame of the ^{19}F shielding tensor. (Figure appears in color online.)

δ_{ii} ($i = x$, y or z) are the components of the ^{19}F chemical shift tensor defined in the principal order frame (shown in Fig. 6 for KS2). In Table 2 we reported the values of the principal components (i.e., defined in its principal axes frame) of the traceless chemical shift tensor, δ_{ii}^0, calculated for the different samples applying the different strategies "VACUO Mod", "VACUO" and "ANISO", previously described in the "Experimental/DFT calculations" section.

Table 2. ^{19}F principal components δ_{ii}^0 of the traceless chemical shift tensors of the investigated compounds, calculated with the different strategies "ANISO", "VACUO" and "VACUO Mod", as explained in the text. $\Delta\delta^0 = \delta_{zz}^0 - (\delta_{xx}^0 + \delta_{yy}^0)/2$. The labeling of fluorine nuclei (F_a and F_b) is that reported in Table 1, while F_{av} indicates an hypothetical fluorine nucleus having CST components obtained by averaging the CST components of F_a and F_b

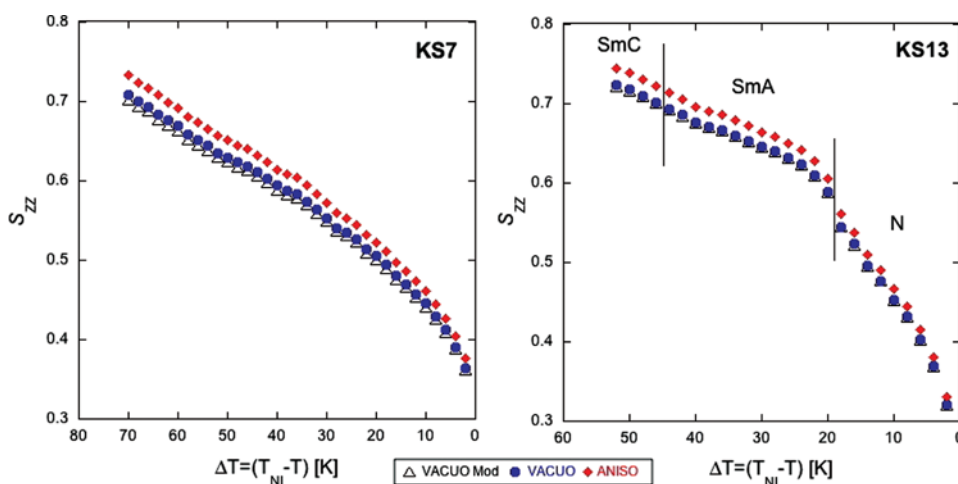|		ANISO				VACUO	VACUO Mod
		δ_{xx}^0	δ_{yy}^0	δ_{zz}^0	$\Delta\delta^0$	$\Delta\delta^0$	$\Delta\delta^0$
KS2	F_a	38.5	−108.5	70.0	105.1	108.1	109.6
	F_b	38.5	−108.4	69.9	104.8	108.6	109.2
	F_{av}	**38.5**	**−108.5**	**69.9**	**104.9**	**108.3**	**109.4**
KS7	F_a	38.4	−108.4	70.0	105.0	108.4	109.6
	F_b	38.4	−108.3	69.9	104.8	108.1	109.2
	F_{av}	**38.4**	**−108.3**	**69.9**	**104.9**	**108.3**	**109.4**
KS9	F_a	38.6	−108.2	69.7	104.5	108.5	107.4
	F_b	39.9	−109.4	69.4	104.2	109.0	108.2
	F_{av}	**39.2**	**−108.8**	**69.6**	**104.3**	**108.8**	**107.8**
	F_a	42.0	−107.9	65.9	98.9	101.9	100.6
KS12	F_b	38.6	−107.1	68.6	102.8	106.3	108.2
	F_{av}	**40.3**	**−107.5**	**67.2**	**100.8**	**104.1**	**104.4**
	F_a	42.1	−108.2	66.1	99.2	102.1	100.6
KS13	F_b	38.7	−107.4	68.7	103.1	106.3	108.2
	F_{av}	**40.4**	**−107.8**	**67.4**	**101.1**	**104.2**	**104.4**

Figure 7. Trends of the principal orientational order parameter, S_{zz}, versus ΔT [K] for KS7 (left) and KS13 (right). The values were derived by employing ^{19}F chemical shift tensors calculated by using the "VACUO Mod", "VACUO" and "ANISO" approaches, as explained in the text. (Figure appears in color online.)

Since in all cases the principal axes frame of the ^{19}F chemical shift tensor resulted almost coincident with the principal order frame (see Fig. 6), and since $\Delta\delta = \delta_{zz} - (\delta_{xx} + \delta_{yy})/2$ does not change when we change the reference of the chemical shift scale, the $\Delta\delta^0$ values reported in Table 2 were used for $\Delta\delta$ of equation (3).

Figure 7 illustrates the trends with temperature of the principal orientational order parameter, S_{zz}, obtained for KS7 and KS13 as described above, using the three different calculation strategies ("VACUO Mod", "VACUO" and "ANISO") reported in the experimental section. We can easily notice that, for both liquid crystals (but the results hold true also for the other three liquid crystals), the values of S_{zz} progressively increase going from the "VACUO Mod", to the "VACUO" to the "ANISO" case, as a consequence of the corresponding decrease of $\Delta\delta^0$. It is quite clear that the effect of considering the whole aliphatic chains rather than a methyl group on either $\Delta\delta^0$ or S_{zz} is almost negligible, while the replacement of calculations "in vacuo" with those, more sophisticated, "in the medium" brings to a detectable increase of the derived S_{zz} values, which however is always less than 5%.

4. Discussion

The orientational order parameters determined for the five liquid crystals here investigated by the optical method and by dielectric and ^{19}F NMR spectroscopies are reported and compared in Figures 8(a) and 9(a).

It is quite clear that the three different approaches here used to determine orientational order parameters present some noticeable differences. These mostly concern the different anisotropic physical quantities measured and, consequently, the different axis frame in which the order parameters are defined. Dielectric and optical methods measure whole-molecule quantities, allowing molecular order parameters defined in the polarizability and dielectric tensor principal axes frames, respectively,
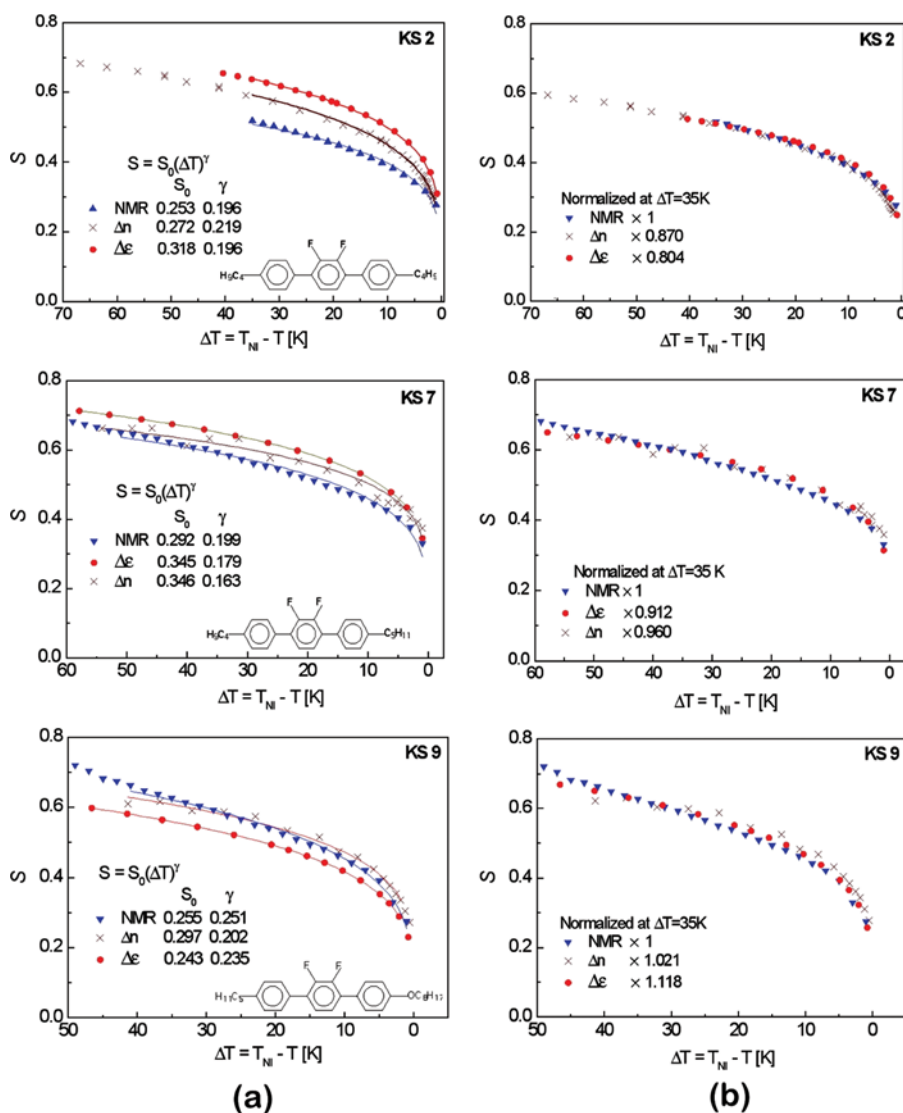
Figure 8. Principal order parameter S_{zz} *vs.* shifted temperature ΔT [K], before (a) and after (b) normalization to the NMR value at $\Delta T = 35$ K for KS2, KS7 and KS9 compounds determined from optical method, dielectric and NMR spectroscopies, as explained in the text, and fits to the Haller-type relation [16]. Chemical structures, fitting parameters and normalization factors are reported in the insets. (Figure appears in color online.)

to be determined. On the other hand, NMR properties rely on local orientational order parameters that can be referred to molecular fragments (in our case to the fluorinated phenyl fragment), and eventually to ''molecular'' order parameters.

All this considered, the experimental data obtained from the three methods show a good agreement. Indeed, the main differences consist in a shift of S_{zz} values, which can be mostly ascribed to the different reference frame in which the order parameters are defined in the three cases, but the trends with temperature show a very similar
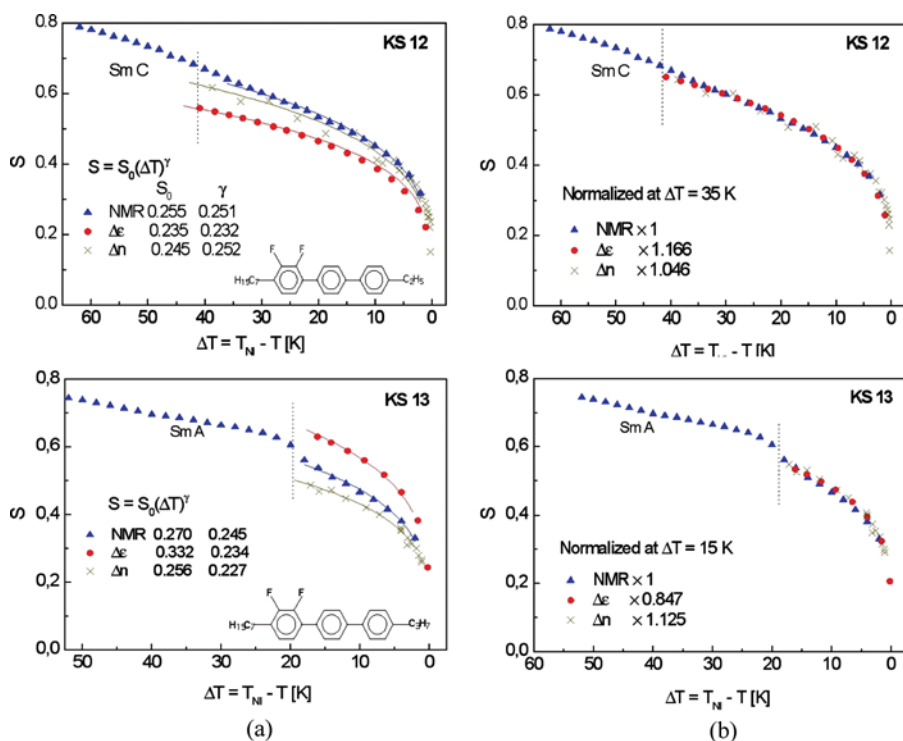
Figure 9. Principal order parameter S_{zz} vs. shifted temperature ΔT [K] of KS12 and KS13 compounds, before (a) and after (b) normalization to the NMR value at $\Delta T = 35$ K (KS12) or 15 K (KS13) determined from optical method, dielectric and NMR spectroscopies, as explained in the text, and fits to the Haller-type relation [16]. Chemical structures, fitting parameters and normalization factors are reported in the insets. (Figure appears in color online.)

behavior. In order to highlight this aspect, and in agreement with what previously done on different liquid crystals [3–5] we have "normalized" the data obtained by optical methods and dielectric spectroscopy to those derived by NMR. The results, shown in Figures 8(b) and 9(b), clearly indicated a very good agreement of the trends obtained by the three techniques.

For all the sets of data the trend of the order parameter with temperature was also fitted to the Haller-type relation [16]

$$S(T) = S_0(\Delta T)^{\gamma} \tag{4}$$

where $S_0 = 1/T_{NI}^{\gamma}$ and $\Delta T = T_{NI} - T$ is the shifted temperature. The results of the fits are reported in Figures 8(a) and 9(a). Quite similar γ values were obtained for the orientational order parameters trends obtained by the three different experimental approaches, with a maximum deviation of 0.05 observed for KS9 between dielectric and NMR spectroscopies. The values obtained for γ are typical of nematogens, with average values ranging from about 0.18 in KS7 to 0.24–0.25 in KS12 [1,3–5,8].

4. Conclusions

The three experimental techniques employed in determining the orientational order parameter in the nematic phase of compounds exhibiting the negative dielectric anisotropy yielded different $S(T)$ – values, Figures 8(a) and 9(a). This is understandable because each of them is related to different molecular observables and reference frames. It is no doubt, however, that the NMR techniques, enriched by quantum mechanical calculations, lead to the most reliable quantities. Therefore, a good consistency of the normalized data obtained by ''more rough'' methods (dielectric and optical anisotropies) and the ^{19}F NMR spectroscopy, presented in Figures 8(b) and 9(b), indicates that the basic assumptions (mainly the local field models) on which the first two methods are based upon reflect fairly well the temperature trends in the nematic order parameter.

Appendix

Determination of Polarizability Anisotropy From Birefringence Measurements

The molecular polarizability can be determined from optical measurements assuming a local field model. In the simplest case of isotropic local field, introduced by Vuks [18], the polarizability components $\alpha_\parallel$ and $\alpha_\perp$ of an optically uniaxial medium can be calculated from equations:

$$\frac{n_e^2 - 1}{\langle n^2 \rangle + 2} = \frac{4\pi\rho\alpha_\parallel}{3N_A M} \tag{A1}$$

$$\frac{n_o^2 - 1}{\langle n^2 \rangle + 2} = \frac{4\pi\rho\alpha_\perp}{3N_A M}. \tag{A2}$$

In the above equations N_A denotes the Avogadro number, M – the molar mass, ρ – mass density, n_o and n_e – ordinary and extraordinary refractive indices, $\langle n^2 \rangle$ – the mean value of refractive indices ($\langle n^2 \rangle = (2n_o + n_e)/3$). It is clear from equations (A1) and (A2) that for determination of principal polarizability components both refractive indices n_o, n_e and density ρ must be known. The same is valid for the polarizability anisotropy $\Delta\alpha = \alpha_\parallel - \alpha_\perp$ [8]:

$$\Delta n \equiv n_e - n_o = \frac{4\pi N_A \rho}{3M} \cdot \frac{\langle n^2 \rangle + 2}{n_e + n_o} \cdot \Delta\alpha \tag{A3}$$

Obviously, the knowledge of birefringence is not sufficient and both indices must be measured. We will try to omit this demand. After expressing the ''optical'' factor $B \equiv (\langle n^2 \rangle + 2)/(n_o + n_e)$ by the set of variables Δn, $\langle n^2 \rangle$ we obtain:

$$\Delta n = \frac{4\pi N_A \rho}{3M} \cdot B \cdot \Delta\alpha \tag{A4}$$

with

$$B = \frac{3(\langle n^2 \rangle + 2)}{2\sqrt{9\langle n^2 \rangle - 2(\Delta n)^2} + \Delta n} \tag{A5}$$
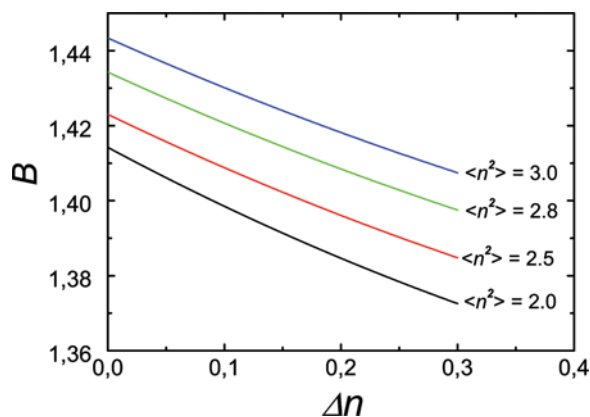
Figure A1. Dependence of "optical" factor B on birefringence for typical values of the mean refractive index and Δn. (Figure appears in color online.)

The $B(\Delta n)$ dependence is shown in Figure A1. As Figure A1 demonstrates, the influence of the parameter $<n^2>$ on B is rather weak (about $\pm 1.5\%$). The temperature changes of B are also negligible. Moreover, these changes are opposite to density changes (typically $\Delta\rho/\rho = 10^{-3}$/kelvin [19–22]). Therefore in further calculations we assume $B = 1.4$ and neglect the temperature dependence of the product $\rho \cdot B$. Despite this, the temperature dependence of $\Delta\alpha$ should be correctly reproduced.

To calculate the polarizability anisotropy also the density ρ must be known. For most calamitic liquid crystals its value ranges from $0.9\,g/cm^3$ to $1.1\,g/cm^3$ [19–22]. We assume $\rho = 1\,g/cm^3$. The error in estimation of the absolute value of polarizability anisotropy does not exceed $\pm 10\%$.

The anisotropy of polarizability estimated in the described way for all materials investigated in this work are shown in Figure A2.
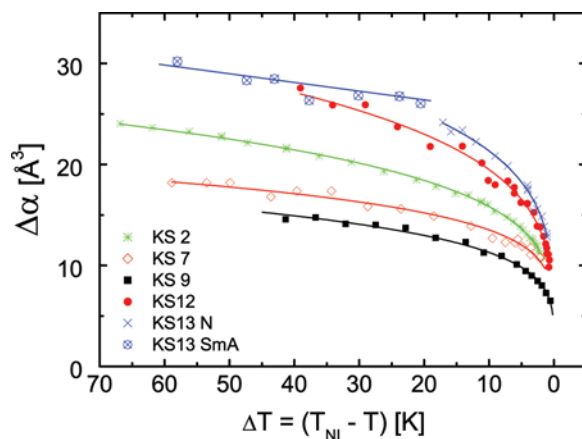

Figure A2. Polarizability anisotropy of investigated terphenyls as function of temperature. (Figure appears in color online.)

References

[1] Urban, S., Würflinger, A., & Gestblom, B. (1999). *Phys. Chem. Chem. Phys.*, *1*, 2787, and references therein.

[2] Domenici, V., Geppi, M., & Veracini, C. A. (2007). *Progr. Nucl. Magn. Reson. Sp.*, *50*, 1, and references therein.

[3] Catalano, D., Geppi, M., Marini, A., Veracini, C. A., Urban, S., Czub, J., Kuczyński, W., & Dąbrowski, R. (2007). *J. Phys. Chem. C*, *111*, 5286.

[4] Geppi, M., Marini, A., Veracini, C. A., Urban, S., Czub, J., Kuczyński, W., & Dąbrowski, R. (2008). *J. Phys. Chem. B*, *112*, 9663.

[5] Borsacchi, S., Calucci, L., Czub, J., Dąbrowski, R., Geppi, M., Kuczyński, W., Marini, A., Mennucci, B., & Urban, S. (2009). *J. Phys. Chem. B*, *113*, 15783.

[6] Kula, P., Spadło, A., Dziaduszek, J., Filipowicz, M., Dąbrowski, R., Czub, J., & Urban, S. (2009). *Opto-Electron. Rev.*, *16*, 379.

[7] Urban, S., Kula, P., Spadło, A., Geppi, M., & Marini, A. (2010). *Liq. Cryst.*, *37*, 1321.

[8] Kuczyński, W., Żywucki, B., & Małecki, J. (2002). *Mol. Cryst. Liq. Cryst.*, *381*, 1.

[9] Frisch, M. J., *et al.* (2009). *Gaussian 09 Revision A01*, Gaussian, Inc.: Wallingford, CT.

[10] (a) Becke, A. D. (1993). *Chem. Phys.*, *98*, 1372; (b) Lee, C., Yang, W., & Parr, R. G. (1988). *Phys. Rev. B*, *37*, 785.

[11] Cances, E., Mennucci, B., & Tomasi, J. (1997). *J. Chem. Phys.*, *107*, 3032.

[12] Casewit, C. J., Colwell, K. S., & Rappe, A. K. (1992). *J. Am. Chem. Soc.*, *114*, 10046.

[13] Ditchfield, R. J. (1972). *Chem. Phys.*, *56*, 5688.

[14] Perdew, J. P., Burke, K., & Wang, Y. (1996). *Phys. Rev. B*, *54*, 16533.

[15] Adamo, C., & Barone, V. (1998). *J. Chem. Phys.*, *108*, 664.

[16] Haller, I. V. (1975). *Prog. Solid State Chem.*, *10*, 103.

[17] Maier, W., & Meier, G. (1961). *Z. Naturforsch. A*, *16*, 262.

[18] Vuks, M. F. (1960). *Optika i Spektroskopiya*, *20*, 651.

[19] Dunmur, D. A., & Miller, W. H. (1979). *J. Phys. (Paris)*, *40*, C3-141.

[20] Kelker, H., & Hatz, R. (1980). *Handbook of Liquid Crystals*, Verlag Chemie: Weinheim, Deerfield.

[21] Kuss, E. (1981). *Mol. Cryst. Liq. Cryst.*, *76*, 199.

[22] Würflinger, A., & Sandmann, M. (2001). In: *Equation of state in nematics*, Physical properties of liquid crystals, Nematics, EMIS Datareview Series, vol. 25, Dunmur, D. A., Fukuda, A., & Luckhurst, G. R. (Eds.), Institution of Electrical Engineers: London, p. 151.